Earth Reinforcement, Ochiai, Yasufuku & Omine (eds) © 1996 Balkema, Rotterdam. ISBN 90 5410 833 9

Effect of normal pressure and width of geosynthetic horizontal drain in pullout behaviour using saturated clay

Tej B.S. Pradhan, Dinesh R. Shiwakoti & Goro Imai
Department of Civil Engineering, Yokohama National University, Japan

ABSTRACT: Geosynthetic horizontal drain (GHD) of widths 50-150 mm has been subjected to laboratory pullout tests at 30-150 kPa normal pressures to study the interface interaction behaviour between saturated clay and GHD. Three types of failure mechanisms namely pullout failure, tension failure and compound failure have been identified depending on normal pressure and GHD width. Consolidation characteristics, local deformation of GHD, shear force and shear stress distribution patterns have been examined.

1 INTRODUCTION

Geosynthetics are superior to steel in reinforcing cohesive soils. Although polymer geogrid performs better than steel in reinforcing clayey soils (Ingold & Templemen, 1977), neither of them have drainage ability. Geosynthetics with high transmissivity, permittivity, strength and stiffness are the ideal reinforcing materials when it comes to constructing saturated or nearly saturated clay embankments. Reinforcement in addition to the strength increase due to drainage is expected from such materials. Geosynthetic horizontal drain (GHD) is the appropriate terminology for grouping these materials whose one of the main functions is drainage of water in lateral direction as in clay embankments.

Tatsuoka et. al. (1986, 1987) examined the short and long term performance of several clay embankments reinforced with non-woven geotextiles and concluded that geotextiles are very effective in draining excess pore water pressure in addition to achieving better compaction control and tensile soil reinforcement. Farina (1990) studied geotextile reinforced clay wall models and found that high transmissivity geosynthetics drastically improve the drainage characteristics leading to increase in undrained shear strength of cohesive backfills. Kamon et. al. (1994) constructed soft clay embankments with various GHDs to investigate the short and long term effects. They concluded that GHDs can be used successfully to construct soft clay embankments. It can be said that soft clay embankments or walls with appropriate GHDs have promising future prospect.

However, experimental research on interaction behaviour between clay and GHDs is rare in literature. Pradhan et. al. (1996) studied pullout behaviour of five different types of GHDs having wide range of strength stiffness and shape using saturated clay. In this research, mainly the effect of normal pressure and GHD width in pullout behaviour will be examined.

2 EXPERIMENTAL PROGRAM

2.1 Materials used

Soft clay recovered from Tokyo Bay is completely reconstituted by seiving it through 75 micron seives, making slurry from the fines with consistency of twice the liquid limit and preconsolidating the slurry at 50 kPa normal pressure in mold of diameter 300 mm × 320 mm height. At the end of preconsolidation, the height of the sample thus prepared is about 15 cm, its water content being about 60% and degree of saturation almost 100%. Gs, LL and PI of the clay are 2.65, 74% and 44 respectively. Soil block of 245 mm × 160 mm × 100 mm thickess is cut from it and is divided into two, lower part being 55 mm and upper part 45 mm thick.

GHD having weavy or undulated core (sheet thickness 0.5 mm) and non-woven geotextile as filter cover with total nominal thickness 10 mm and widths of 50, 75, 100 & 150 mm is tested, and the one used here corresponds to Type C of five various GHDs tested by Pradhan et. al. (1996). Method of preparing GHD specimen is also the same.

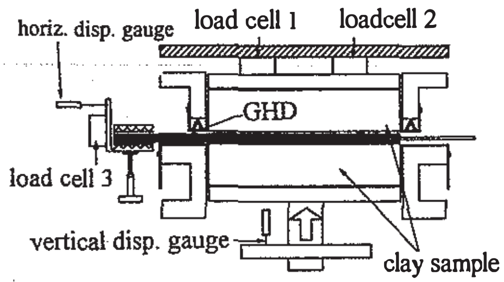

(a) longitudinal section

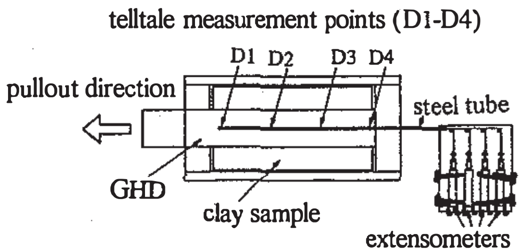

(b) details of displacement measurement system

Fig. 1 Pullout Appratus

2.2 Pullout apparatus

Pullout box with inner dimension 246 mm length, 160 mm width and 100 mm thickness is used (Fig. 1). Two load cells each having capacity of 10 kN are stationed right below the reaction frame to measure the average normal load applied at clay-GHD interface. A load cell of capacity 10 kN is used to measure pullout force. Displacements are measured at four selected locations along the embedded length of GHD, through flexible steel wires of dia. 0.27 mm. These wire systems are referred to as telltales.

2.3 Test program and procedure

Testing conditions and results are summarised in Table 1. Average normal pressure σ_n is kept constant throughout the test. Pullout tests have been carried out at the end of primary consolidation. Embedded length of GHD is 245 mm for all tests. Pullout tests have been conducted at the displacement rate of 1 mm/min.

3 RESULTS AND DISCUSSIONS

3.1 Consolidation behaviour

The effectiveness of GHD and the role of its width in reducing consolidation time can be seen clearly from Fig. 2. The larger the width the smaller the drainage path, hence shorter the duration to achieve the end of the primary consolidation.

Fig. 3 compares the water content variation across the sample before consolidation and at the end of pullout.

Table 1 Summary of pullout tests and results

GHD width cm	σ_n kPa	P_{max} kN/m	τ/σ at P_{max}	η(%)	δ_{h1} at P_{max} mm	e_0	e_f	Failure Mode
5	30	8.36	0.57	93	3.4	1.57	1.54	P
5	50	13.35	0.55	90	12.2	1.48	1.42	P
5	70	18.08	0.53	87	12.1	1.56	1.39	C
5	100	15.20	0.31	54	14.7	1.68	1.46	T*
5	150	23.92	0.33	56	1.5	1.68	1.42	T*
7.5	50	13.50	0.56	91	13.4	1.60	1.46	C
10	30	7.41	0.52	85	8.8	1.57	1.46	P
10	50	14.55	0.60	97	-	1.55	1.39	T
10	70	19.02	0.56	92	19.3	1.61	1.38	C
10	150	18.66	0.26	45	6.9	1.49	1.22	T*
15	30	9.02	0.63	100	10.6	1.51	1.46	P
15	50	14.45	0.60	97	20.3	1.59	1.49	T
15	70	18.45	0.54	89	16.8	1.59	1.44	T
15	100	12.64	0.26	45	14.7	1.54	1.34	T*

T: tension failure; C: compound failure; P: pullout failure; T*: premature tension failure; P_{max} : maximum pullout force; δ_{h1}: telltale displacement at D1 (see Fig. 1); η: Efficiency = Φ_{IF} / Φ_{clay}, $\Phi_{IF} = \tan^{-1}[\tau_{max}/\sigma_n]$, $\Phi_{clay}=32°$ e_o & e_f: initial and final void ratios

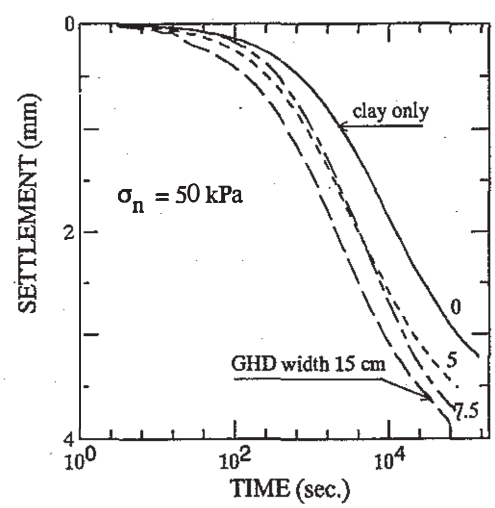

Fig. 2 Consolidation Duration and GHD Width

Low water content in the vicinity of geosynthetics was also reported by Fabian (1987) in clay model wall test using geotextile. Reduction in water content is higher towards front end compared to that at rear end along the longitudinal section. During shearing, the concentrated shear stress towards front end is mainly responsible for it. This decrease in water content during pullout causes additional increase in interface frictional resistance.

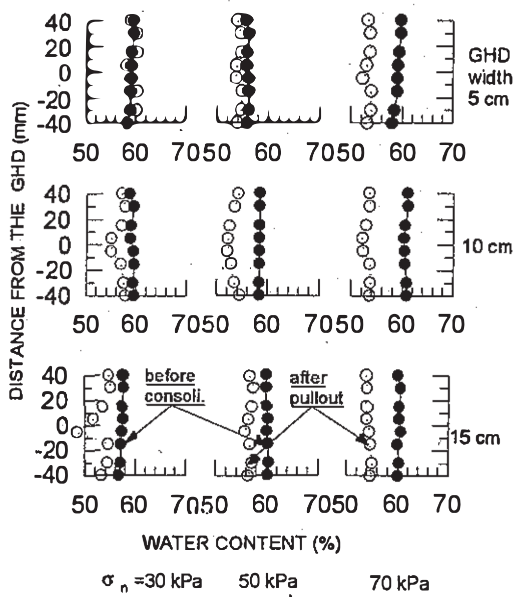

Fig. 3 Water Content Distribution across GHD

3.2 Failure mechanisms

Failure pattern depends on strength, stiffness and shape of GHD as well as the applied normal pressure for a given soil type (Pradhan et. al. 1996). For a given GHD and soil type, three distinct types of failure modes have been identified based on the applied normal pressure and width of GHD (Figs. 4 - 6, Table 1). If GHD sheet comes out towards the pulling side excessively, almost equal displacement will occur along its length. This type of failure is *pullout failure* (Fig. 4). Second type is *tension failure* in which filter/core of GHD will break as a result of excessive tension in GHD (Fig. 5). Tension failure may occur at the front end of shear box or near the clamping end. *Compound failure* is the third type of failure and is the combination of the above two. In this category, maximum pullout resistance is mobilised while the GHD is slipping out. During post peak period, filter/core start(s) to tear out leading to sharp decline in pullout resistance (Fig. 6).

At high normal pressures ($\sigma_n \geq 100$ kPa), failure occured due to filter/core breakage outside the pullout box before fully mobilising the pullout shear resistance. As a result, the maximum pullout resistance mobilised in such cases is pseudo-peak. This type of failure is referred as *premature failure* and does not occur in field application. Interpretation of premature failure type test data needs precaution.

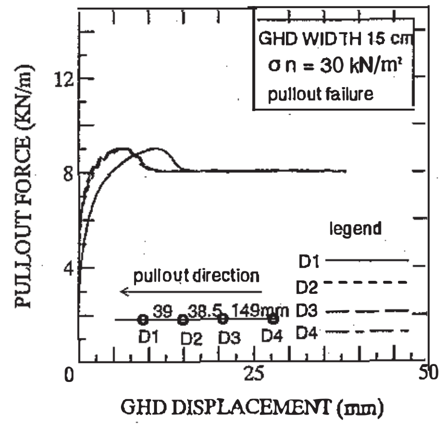

Fig. 4 Typical Pullout Failure

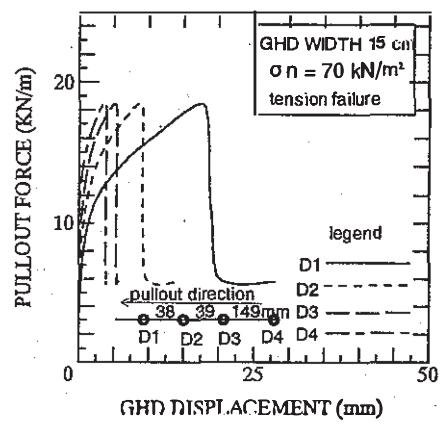

Fig. 5 Typical Tension Failure

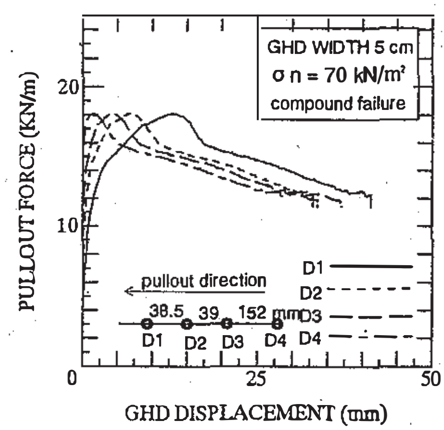

Fig. 6 Typical Compound Failure

3.3 Effect of GHD width and normal pressure in failure mechanism

From data shown in Table 1 & Figs. 4-6, following points may be noted: (1) At very small normal pressure invariably *pullout failure* occurs regardless of GHD width. (2) At medium normal pressure (50-70 kPa), failure mechanism depends on GHD width. If the GHD width is smaller, *pullout failure* or *compound failure* is predominant; however, tension failure is the main mode of failure at large GHD width. (3) At high normal pressure, failure is *tension failure*, regardless of GHD width. (4) Displacement required to mobilise peak shear strength depends on normal pressure and GHD width. Larger the GHD width, longer the displacement required to reach peak. In case of *pullout failure*, which is the case of low to medium normal pressure, displacement at failure is smaller. (5) Except for premature failure, efficiency of clay-GHD interface friction is 85% or more. At larger normal pressure, efficiency is lower. For wider GHD, efficiency is slightly higher.

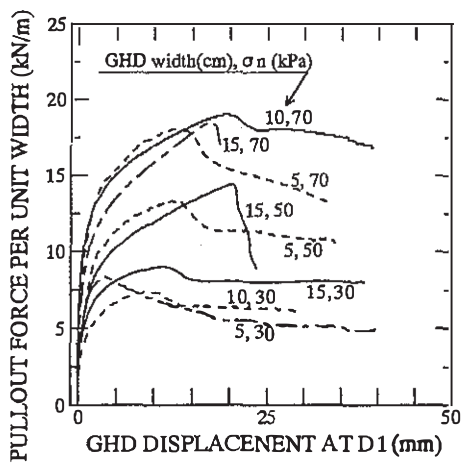

Fig. 7 Effect of GHD Width in Pullout Resistance

Fig. 7 shows plot of pullout force per unit width vs. telltale displacement at front most measured point (D1) for various GHD widths and normal pressures. GHD with 5 cm shows stiffer response compared to larger widths. However, larger peak pullout force is mobilised for the one with larger widths at larger strain.

3.4 GHD deformation

Displacement at any measuring point consists of two parts: rigid body displacement and extension of GHD itself. The incremental displacement between two consecutive measuring points is the net extension of GHD between these points. At very small normal pressure, mainly the rigid body movement occurs. As the normal pressure increases, GHD extension also starts increasing, especially at the front part. Fig. 8 shows the progressive deformation development at σ_n of 30 kPa and 150 kPa. It may be noted that the incremental displacement is larger towards the clamped end which keeps increasing with increase in pullout force. Thus the local deformation is non-linear and its degree depends on normal pressure.

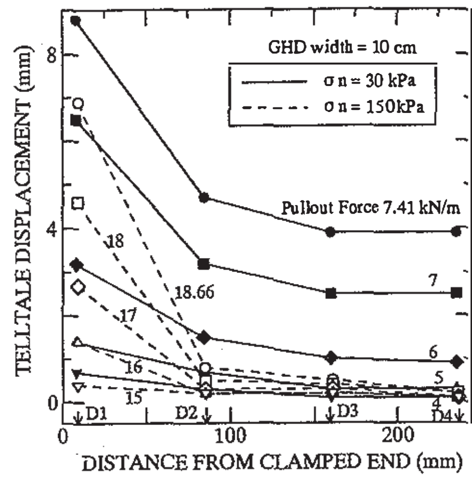

Fig. 8 Effect of Normal Pressure in Local Deformation

3.5 Shear force & shear stress distribution along GHD

Shear force distribution along the embeded length of GHD was estimated using the method suggested by Hayashi et. al. (1994). From the difference between two consecutive telltale displacements, local strain was calculated and from that value, shear force was estimated using the index stress-strain curve obtained by the tensile test of GHD under no lateral confining pressure. Separate index stress-strain curve for the core and filter were converted to tensile force per unit width and superimposed to get the combined effect of core and filter. It should, however, be noted that the properties of core and filter are not elastic and such superimposition cannot reflect true composite behaviour. Thus the results obtained using these curves are only approximate.

Local shear stress distribution at various points along the GHD length were calculated using the shear force difference between two consecutive points and the corresponding contact surface area between the same points.

Fig. 9 shows the shear force developed along GHD length during pullout. Its corresponding shear stress distribution is shown in Fig. 10. It can be seen that at front part of GHD, very large shear stress develops from an early stage of pullout whereas shear stress developed at the rear end is very small even at peak pullout force.

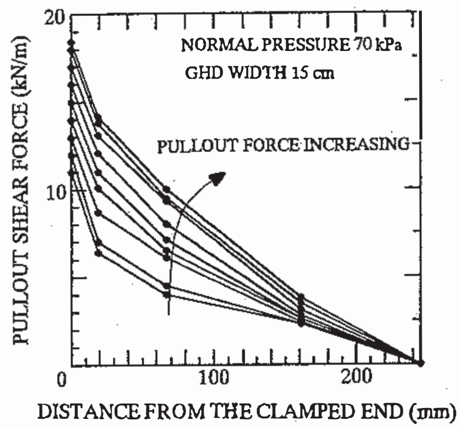

Fig. 9 Shear Force Development During Pullout

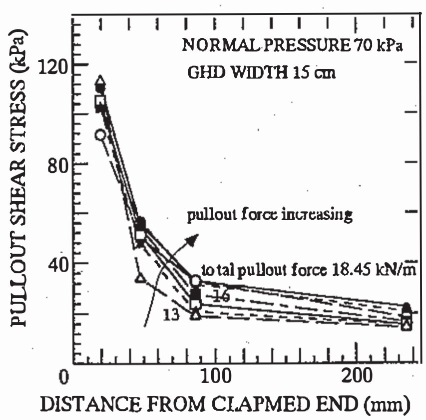

Fig. 10 Shear Stress Development During Pullout

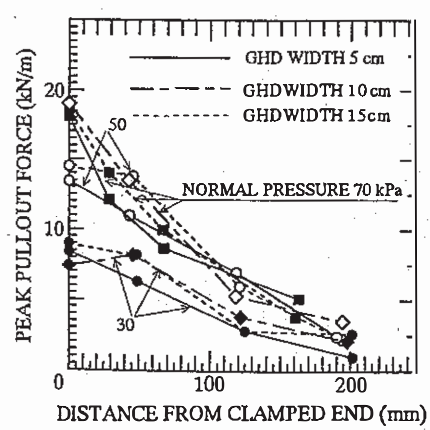

Fig. 11 Comparision of Shear Force Distribution

Comparison of shear force distribution have been made at peak pullout force and 30, 50, & 70 kPa normal pressures in Fig. 11. Except for normal pressure of 30 kPa, all the curves fall within a narrow band implying that GHD width has no significant effect in shear force distribution.

3.6 Effect of width and modulus of GHD in normal stress

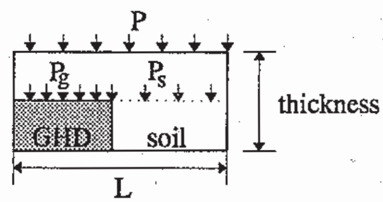

Fig. 12 Forces acting on GHD-soil structures

Refering to the force equilibrium in Fig. 12, total applied normal load (P) = load on GHD (P_g) + load on soil (P_s). i. e., $P/A = P_g/A + P_s/A$. So the total (global) normal stress is

$$\sigma = \left(A_g/A\right)\times\sigma_g + \left(A_s/A\right)\times\sigma_s \qquad (1)$$

From strain compatibility, assuming that total vertical strain in GHD (ε_g) = total vertical strain in soil (ε_S). i. e.

$$\frac{\sigma_g}{E_g} = \frac{\sigma_s}{E_s} \qquad (2)$$

Combining (1) and (2), we get

$$\sigma_g = \frac{\sigma}{A_g/A + \left(1 - A_g/A\right)\times\left(E_s/E_g\right)} \qquad (3)$$

Where *area ratio* (A_g/A) is the ratio of GHD area to the total area, *modulus ratio* (E_g/E_S) is the ratio of modulus of GHD to soil, σ_g is the local normal stress in GHD, σ_S is the local normal stress in soil and σ is the global normal stress.

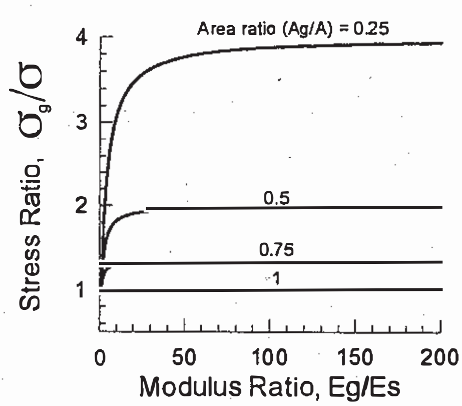

Fig. 13 Effect of Modulus Ratio and Area Ratio

Fig. 13 shows the plot of *stress ratio* against *modulus ratio* using equation 3. It is clear from this figure that modulus ratio and area ratio cannot be neglected in the clay-GHD interface analysis. To avoid the complication in interpretation of test results, it is recommended to test geosynthetics at the same width as the apparatus, whenever possible.

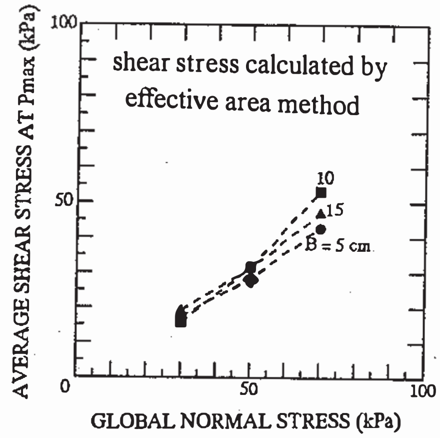

Fig. 14 Failure Envelope with Total Normal Stress

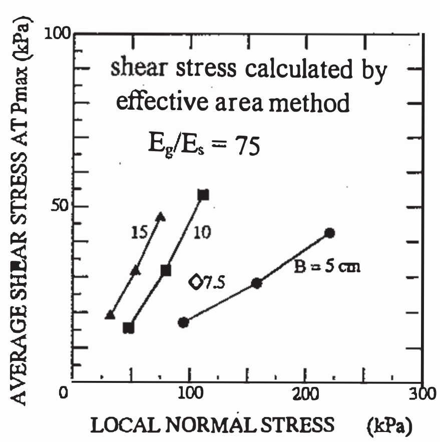

Fig. 15 Failure Envelope with Local Normal Stress

Fig. 14 shows the failure envelope for 50, 100, 150 mm GHD widths. Average shear stress at peak pullout force was calculated using the *effective area method* (Ochiai et. al., 1992). However, the points calculated using total area method were also almost the same. Practically no significant effect of GHD width in failure envelope can be seen. However, if the local normal stress (σ_g) is taken into account, the failure envelope depends on width as shown in Fig. 15. Detailed investigation in needed to clarify this difference.

4 CONCLUSIONS

The following main conclusions can be drawn from the present research.

1) Three types of failure mechanisms (namely pullout failure, tension failure and compound failure) exist as a function of applied normal pressure and GHD width. Premature failure may occur at very large normal pressure.

2) Pullout force per unit width is practically the same for all widths when global normal stress, σ is used. However, if local normal stress on GHD is estimated under elasticity assumption, effect of *modulus ratio* and *area ratio* on pullout shear stress is clearly observed.

3) Local deformation and hence the shear stress distribution is non-linear and is very high at front side. The degree of non-linearity increases both with pullout force and applied normal pressure.

REFERENCES

Fabian, K. (1990). "Time dependent behaviour of geotextile reinforced clay walls", *Pro. of the 4th international conference on Geotextiles, Geomembranes and Related Products*, Vol. 1, ,33-38, Balkema, Rotterdam.

Hayashi, S., Makiuchi, K., Ochai, H. (1994). Testing methods for soil-geosynthetic frictional behaviour-Japanese standard, *Proc. 5th international conference on Geotextiles, Geomembranes and Related Products*, 411-414, Balkema, Rotterdam.

Ingold T. S., and Templeman, L. E. (1977). The comparative performance of polymer net reinforcement. *Proc. Int. Conf. on use of fabrics in geotechniques*, Paris 1: 65-70

Kamon, M., Akai, T., Fukuda, M & Yaida, O. (1994). "Reinforced embankment using geosynthethc horizontal drains", *Proc. 5th international conference on Geotextiles, Geomembranes and Related Products*, 791-794, Balkema, Rotterdam.

Ochiai, H., Hayashi, S., Othani, J., Hirai T. (1992). Evaluation of pullout-resistance of geogrid reinforced soils, *Proc. Int. Symposium on eatrth reinforcement practice*, Fukuoka, Kyusu, Japan (ed. Ochai, Hayashi & Othani), 141-146, Balkema, Rotterdam.

Pradhan, T. B. S., Shiwakoti, D. R., Okamoto, M., Ikedo, S. (1996). Pullout behaviour of geosynthetic horizontal drains in saturated clay, *12th South East Asian Geotechnical Conference*, Malasyia.

Tatsuoka, F., & Yamauchi, H. (1986). "A reinforcing method for steep clay slopes using a non-woven geotextile", *Geotextiles and Geomembranes*, 4, 241-268.

Yamauchi, H., Tatsuoka, F., Nakamura, K., Tamura Y. Iwasaki, K. (1987). Stability of steep clay embankments reinforced with a non-woven geotextile, *Proc. of the post Vienna conf. on Geotextiles*, Singapore, pp 387-403.